AD-A079 983 ARACOR SUNNYVALE CA F/G 20/8
PHOTOEMISSION YIELDS AT LOW X-RAY ENERGIES.(U)
OCT 79 M J BERNSTEIN F49620-78-C-0092
UNCLASSIFIED ARACOR-TR-20-1 AFOSR-TR-79-1327 NL

END
DATE FILMED
2-80
DDC

PHOTOEMISSION YIELDS AT LOW X-RAY ENERGIES

ANNUAL TECHNICAL REPORT FOR
CONTRACT F49620-78-C-0092

ARACOR TECHNICAL REPORT: TR-20-1
October 30, 1979

Prepared for:

AIR FORCE OFFICE OF SCIENTIFIC RESEARCH
Attention: NP
Building 410
Bolling AFB, DC 20332

SECURITY CLASSIFICATION Unclassified

REPORT DOCUMENTATION PAGE

READ INSTRUCTIONS BEFORE COMPLETING FORM

1. REPORT NUMBER: AFOSR-TR-79-1327	2. GOVT ACCESSION NO. / 3. RECIPIENT'S CATALOG NUMBER
4. TITLE (and Subtitle): Photoemission Yields at Low X-Ray Energies	5. TYPE OF REPORT & PERIOD COVERED: Annual Technical Report 78 May 1 - 79 Sept 30
	6. PERFORMING ORG. REPORT NUMBER
7. AUTHOR(s): M. J. Bernstein	8. CONTRACT OR GRANT NUMBER(s): F49620-78-C-0092
9. PERFORMING ORGANIZATION NAME AND ADDRESS: ARACOR, 1223 East Arques Avenue, Sunnyvale, CA 94086	10. PROGRAM ELEMENT, PROJECT, TASK AREA & WORK UNIT NUMBERS: 2301/A5, 61102F
11. CONTROLLING OFFICE NAME AND ADDRESS: AFOSR/NP, Bolling AFB, Wash DC 20332	12. REPORT DATE: Oct 1979
	13. NUMBER OF PAGES: 16
14. MONITORING AGENCY NAME & ADDRESS (if different from Controlling Office): Annual Technical Rept. 1 May 78 - 31 Sept 79	15. SECURITY CLASS. (of this report): Unclassified
	15a. DECLASSIFICATION/DOWNGRADING SCHEDULE

16. DISTRIBUTION STATEMENT (of this Report)

Approved for public release; distribution unlimited.

ARACOR-TR-79-1

17. DISTRIBUTION STATEMENT (of the abstract entered in Block 20, if different from Report)

18. SUPPLEMENTARY NOTES

19. KEY WORDS (Continue on reverse side if necessary and identify by block number)

Photoemission
X-rays
Surface Effects
Electron Emission
Primary Electrons
Secondary Electrons

20. ABSTRACT (Continue on reverse side if necessary and identify by block number)

Photoelectron emission parameters have been studied using x radiation in the 1 to 6 keV range. A retarding-potential analyzer was developed to determine the yields of primary electrons about 50 eV and secondary electrons below 50 eV. Yields were measured at eight monochromatic x-ray energies using photoemitting surfaces of gold, silver,

DD FORM 1 JAN 73 1473

UNCLASSIFIED

SECURITY CLASSIFICATION OF THIS PAGE (When Data

20. (Continued)

aluminum, titanium, silicon, deposited graphite, glass, anodized aluminum, Mylar and Saranwrap. The primary yields agreed well with previous results for Au, Al and Ti. The ratios of primary to secondary yields were highest at the low end of the photon-energy range; at 1.26 keV, these secondary-to-primary ratios ranged from about 6 for the oxides of Al and Si down to only 1.2 for Mylar. Supplementary total yield measurements on the above materials were made using pulsed low-energy x radiation. Studies were begun on measuring and analyzing the energy distribution of primary electrons.

RESEARCH OBJECTIVES

The goals of this program are to measure, model and interpret the characteristics of photoelectron emission generated by low-energy x rays in the 1 - 6 keV range. At these low-energies, electron ranges are quite short so that the surface properties can be very important. The principal quantities being measured are the electron yields, Y, as a junction of photon energy E_x. These yields, in units of electron per photon, are the primary-electron yield, Y_p, where the electron energy is E_e is 50 eV$<E_e<E_x$, and the secondary-electron yield, Y_s, where $E_e<50$ eV. An important aspect of these studies is the influence of surface treatment and coatings on the yield values. To help interpret the results, the energy distributions of primary electrons are being studied and the surface composition is being determined by Auger analysis. Materials of interest include metals, semiconductors, inorganic dielectrics and polymers. The end result will be an improved understanding of the electron transport and energy-loss mechanisms in these materials. On the practical side, the energy-dependent responses of some of these materials have application to plasma diagnostics and SGEMP responses.

STATUS OF RESEARCH EFFORT

During the first year of the program, the studies were divided into the following phases: development of instrumentation to measure the photoemission characteristics, selection and evaluation of materials, measurements of total yields and primary yields, analysis and modeling of yield results, and analysis of primary-electron energy spectra. The results of these studies fall into the categories of primary and secondary electrons.

Experiment: Two instruments have been developed at ARACOR to measure the characteristics of photoelectron emission: a retarding-potential analyzer for determining the yields of primary and secondary electrons, and a magnetic photoelectron spectrometer for determining the energy distribution of primary electrons. The latter instrument is an adaptation of a spectrometer system developed to measure the time-resolved photoelectron energy

spectra generated by pulsed plasma x radiation.

A schematic view of the "birdcage" retarding-potential spectrometer, used to determine primary and secondary yields, is shown in Figure 1 and a photograph of this apparatus is in Figure 2. The net transparency of the wire grid and its support was 98%. The x-ray source was a low-energy, Henke-tube calibration facility developed by Science Applications Incorporated, Sunnyvale, for the Defense Nuclear Agency. The output spectrum from a copper anode operated at 16 kV excited characteristic fluorescent lines at eight energies between 1.26 and 5.41 keV. The fluorescent spectra passed alternately through well-matched Ross filter pairs and the resultant spectral purity was better than 98%; the intensity calibration was within 2%. The photoemission currents were measured on a Keithley 610C picoammeter and displayed on a strip-chart recorder. Measured currents ranged from 10^{-15} to 10^{-12} A and could be determined to within 2% of reading plus 3 x 10^{-16} A. The overall accuracy was judged to be better than 5%, except where limited by signal strength.

During the development of the retarding-potential apparatus, several problems were identified and solved. Energetic electrons emitted from the Ross filters on the x-ray source could travel to the photoemitter and affect the measured currents. This was avoided by placing a deflecting magnet with apertures between the source and the "birdcage" apparatus so only photons reached the photoemitter. Another problem was the migration of secondary electrons and low-energy backscattered electrons from the chamber walls to the photoemitter. These were inhibited by maintaining the photoemitter assembly at -32V relative to the vacuum chamber wall. Back-scattered electrons were also reduced by coating the chamber walls and grid with a low-Z coating of graphite. Calibration experiments showed that secondary emission off the retarding-grid was less than 3% of the primary current. A third potential problem checked out was charge build-up on the dielectric samples. Both calculations and measurements indicated that the surface potential was negligible for the sample thicknesses and x-ray intensities used.

The retarding grid was used to differentiate between the secondary

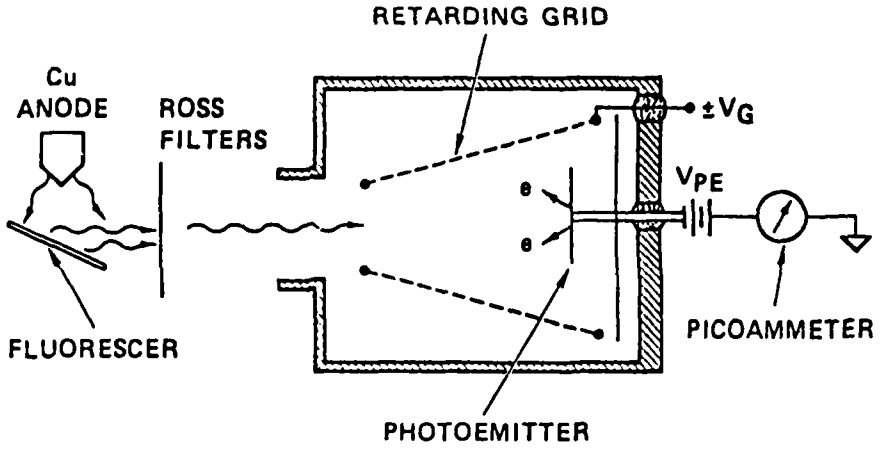

Figure 1. Experimental setup to measure total and primary x-ray photoyields.

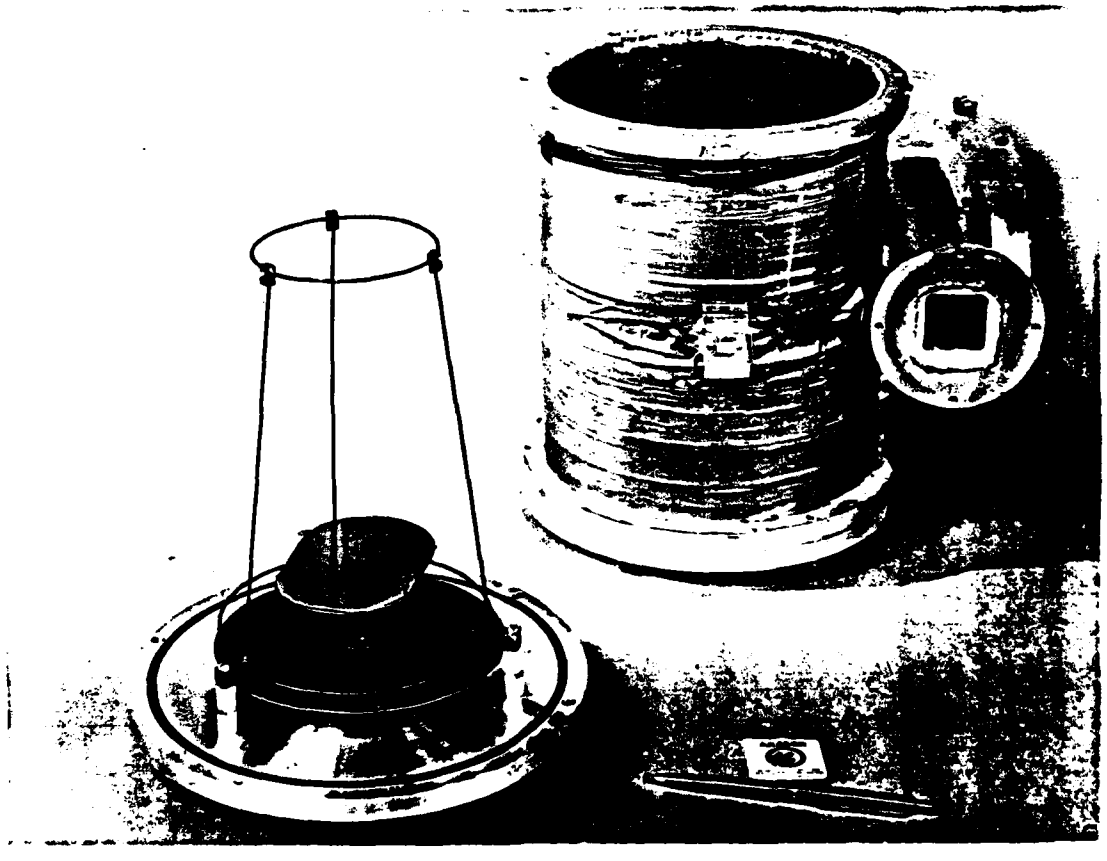

Figure 2. Photograph of "birdcage" retarding potential spectrometer.

electrons and the primary electrons. When the grid was positive with respect to the photoemitter, the total emission was measured, while with the grid sufficiently negative, the net emission is due only to primary electrons. An important aspect in these experiments is the minimum potential between the photoemitter and the chamber walls. On the basis of several computations, the potential of this "escape barrier" was estimated to be 60% of the applied bias. The dependence of the normalized emission current on the grid-to-emitter potential, V_G, is shown in Figure 3 for an aluminum photocathode irradiated by Si-K x rays at 1.74 keV. The total current was constant at all positive voltages and decreased rapidly for small negative values of V_G, corresponding to the energy distribution of low-energy electrons. At negative biases beyond 50 volts, the normalized current exhibited only a gradual decrease.

Figures 4 and 5 are a schematic drawing and a photograph of the magnetic spectrometer that has been developed to measure the energy distribution of primary electrons. Monochromatic x radiation is incident on the beveled photoemitter and a fraction of the emitted photoelectrons pass through the aperture into the spectrometer chamber. In the applied magnetic field, the electrons follow arcs according to their energy. At each setting of the magnetic field, the electrons within a given energy band are collected by the channeltron detector and counted. This instrumentation is an adaptation of a multi-channel photoelectron spectrometer system (PESS) developed to measure the time-resolved photoelectron energy spectra generated by pulsed plasma x radiation.

During this first year, the work on this magnetic spectrometer concentrated on determining the energy calibration and energy resolution through measurements and comparisons with calculations based on electron trajectories. Initial spectral measurements were made using gold and aluminum photoemitters at a few selected x-ray energies.

Material Selection: Photoemission yields from a wide variety of materials were measured during the first year including: metals (gold, silver, titanium, aluminum), semiconductors (silicon, deposited graphite), inorganic insulators (glass, anodized aluminum), and polymers (Mylar, Saranwrap).

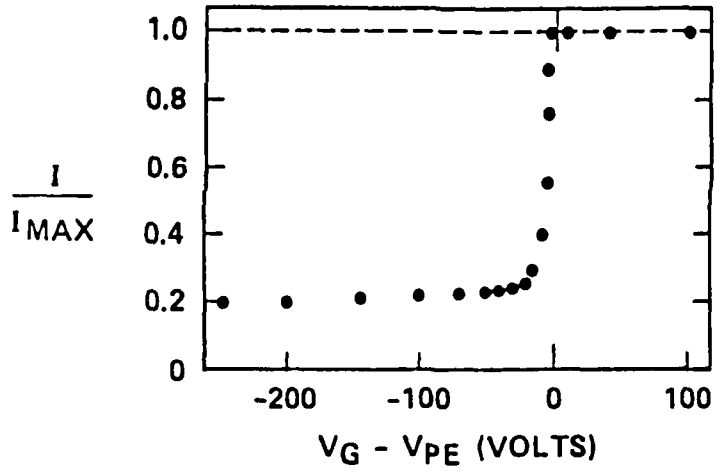

Figure 3. Normalized photoemission current from aluminum as a function of retarding potential; x-ray energy was 1.74 keV.

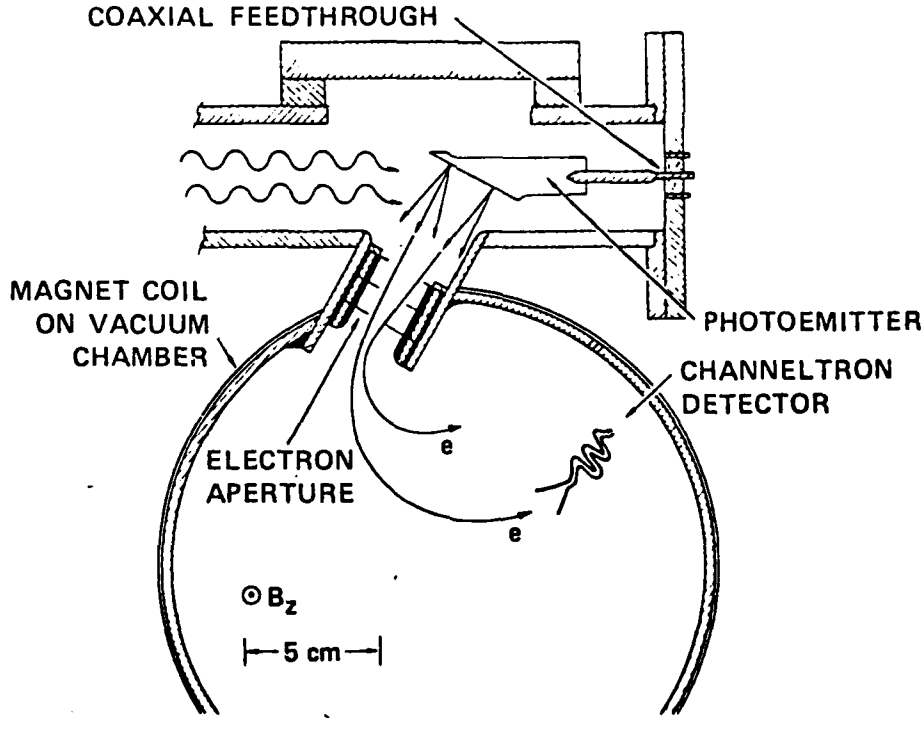

FIGURE 4. PHOTOELECTRON SPECTROMETER SYSTEM USED FOR STEADY-STATE MEASUREMENTS

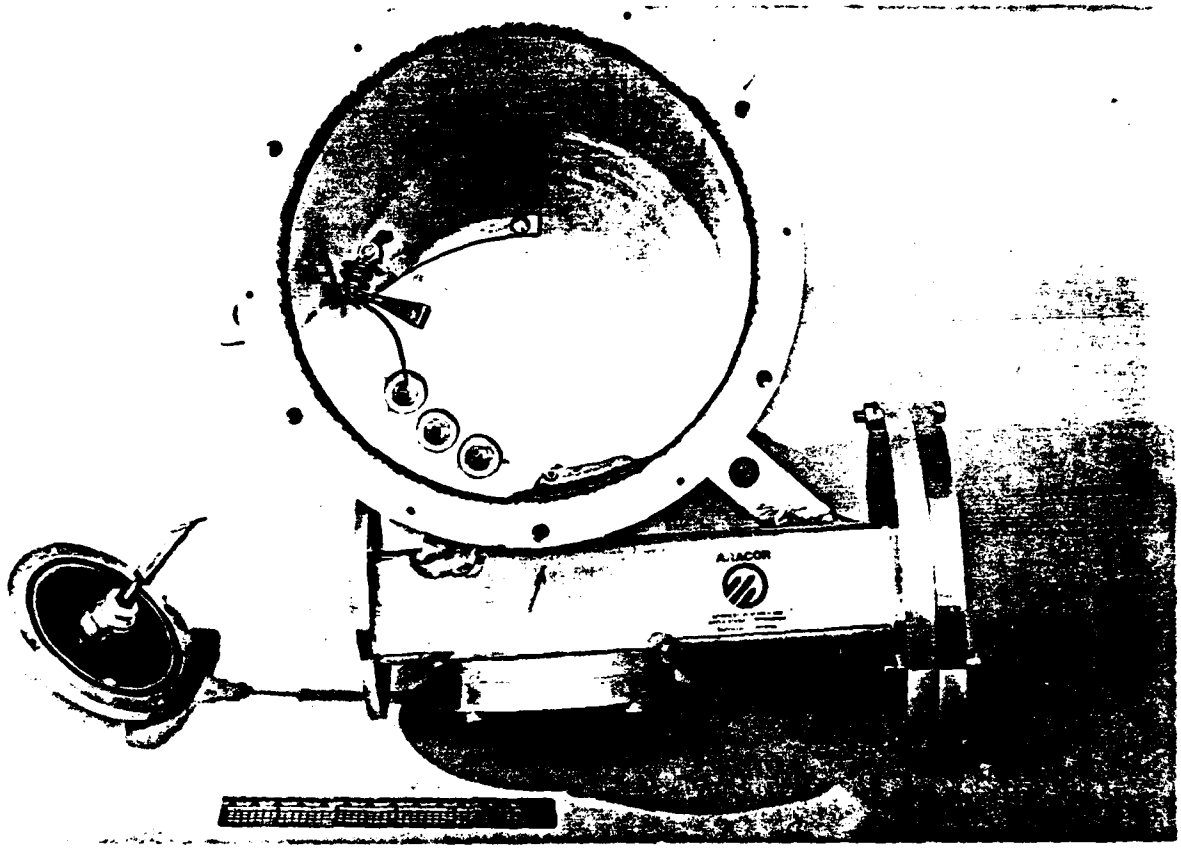

Figure 5. Photograph of magnetic photoelectron spectrometer

Two or three samples of some materials were measured to check reproducibility and the effect of standard cleaning procedures. In accordance with the objectives of this program, all materials were exposed to air before mounting in the vacuum chamber.

In preparation for future measurements, the properties of a large number of different materials were analyzed from the standpoint of obtaining large jumps in the photoyields above the absorption edges of different elements. This objective was to select photocathodes with different energy responses following the criterion of stability when exposed to air. Thus, the materials must be nonhygroscopic and have minimum oxidation. Another criterion is reproducibility in the commercially-available forms or routine processing. Materials (and their predominant absorption edge energies) identified as being of particular interest in this regard included: Zr (L3 at 2.22 keV), Mo (L3 at 2.52 keV), MoS_2 (L3 at 2.52 keV and K at 2.47 keV), W (M5 at 1.81 keV), MgF_2 (K at 1.305 and K at 0.687 keV), CF_2 (K at 0.687 keV and K at 0.284 keV), Ni (L3 at 0.854 keV). Since the photoelectron yield is mainly dependent on the energy-dependent photon absorption, the absorption cross-sections were calculated for various inert compounds containing elements of interest. The objective was to determine how much the jump ratio at the absorption edge of an element was reduced by the combination with another element.

The materials studied in the first year are listed below along with their form, composition and relevant cleaning procedures.

1. Gold: Two samples were used. One was an electroplated gold coating on copper-clad PC board (the irradiated surface was electrically connected to the photoemitter mount). The other sample was gold foil. Both materials were more than a year old. The only cleaning was flushing with reagent-grade methanol.
2. Silver: An electroplated coating on copper-clad PC board. This sample was cleaned with household cleanser and water followed by alcohol flushing. Two sets of measurements were made on this sample--one a day after cleaning and again three days later after opening the vacuum system. There was a detectable, but very small difference in the total yield.

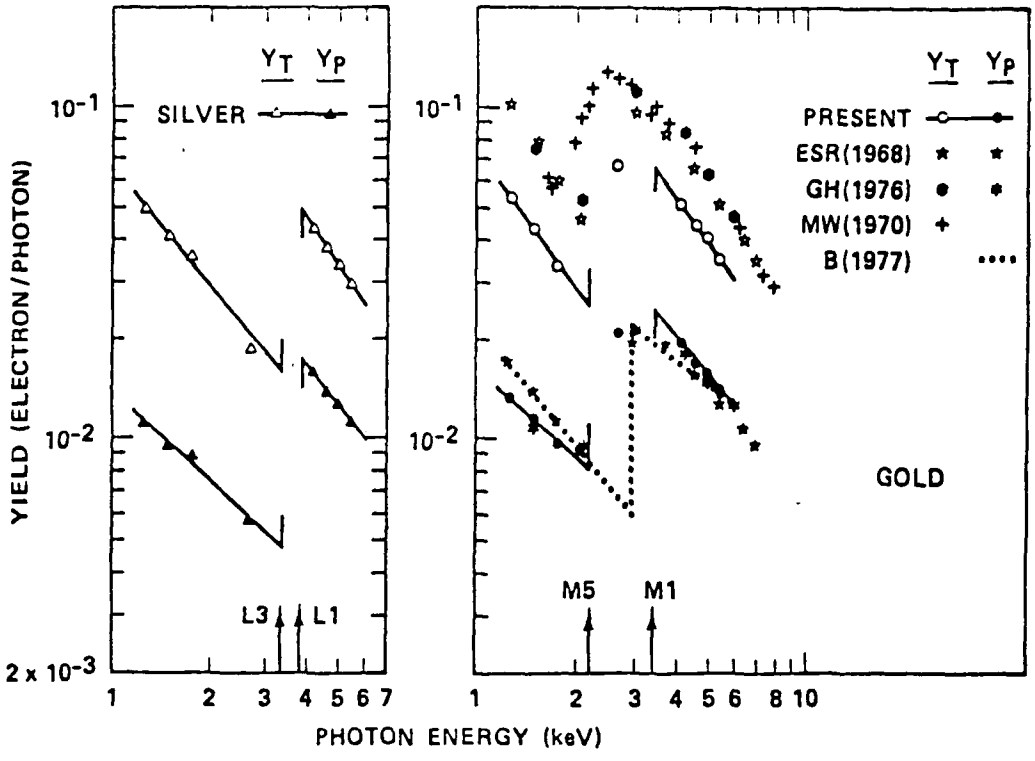

Figure 6. Photoelectron yields from silver and gold.

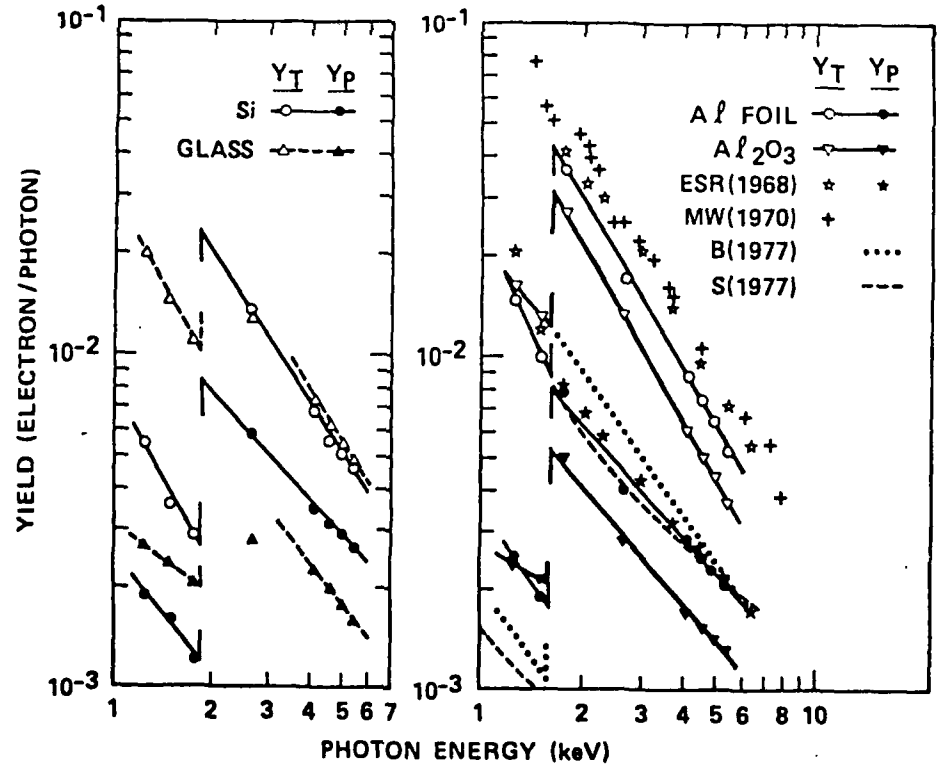

Figure 7. Photoelectron yields from silicon, glass, aluminum foil and anodized aluminum.

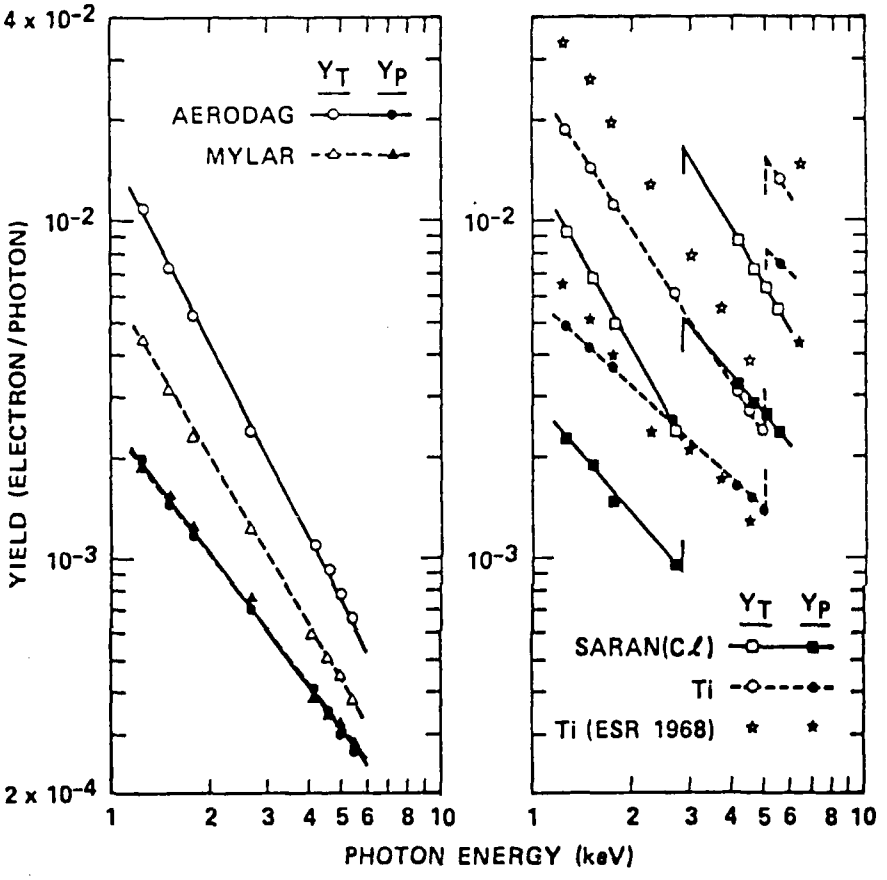

Figure 8. Photoelectron yields from Aerodag (carbon), Mylar, Saran (chlorine) and titanium.

3. Titanium: A foil cleaned with methanol.
4. Aluminum: Standard 18-μm-thick Reynolds Wrap. Several different samples were studied that were mounted fresh from the rolls. All samples had, of course, the normal oxide coating with a thickness of about 4 nm.
5. Aluminum oxide: Standard aluminum foil was anodized in a 3% solution of ammonium citrate. Two samples were prepared using applied voltages of 100 and 200 V to give Al_2O_3 thicknesses of 135 nm and 270 nm.
6. Silicon: A 1-mm thick high-purity wafer of the type used by the semiconductor industry.
7. Glass: Microscope slides 1 mm thick were mounted side by side with a conductive Aerodag backing. The composition was not determined, but the predominant SiO_2 most likely had significant amounts of the normal additives Na_2O, K_2O, and/or CaO.
8. Saran: Commercial 13-μm-thick Saranwrap taken fresh from a roll. Composition is $C_2H_2Cl_2$ plus a small amount of unknown plasticizer. Conductive Aerodag coating on backside.
9. Mylar: Film with thickness of 6 μm taken fresh from a large commercial roll. Composition is $C_{10}H_8O_4$. Aerodag coating put on backside.
10. Carbon: A thick coating of graphite in the form of Aerodag was used.

Results and Analysis: The measured values of total, Y_T, and primary, Y_P, yields from the ten materials are given in Figures 6, 7, and 8. Also given in these figures are: power-law fits through the data of the form $Y = A\ E_X^B$, previously-reported experimental yields for Au, Al and Ti, and previously-reported theoretical yields for Au and Al. The discussion in this section summarizes the noteworthy results and analyses. More details are given in a paper very recently accepted for publication in the IEEE Transactions on Nuclear Science.

There is generally good agreement between the primary yields of Au, Ti and Al and previously-reported results. But the present values for the total yields are lower, by 10 to 40%, than previously reported. It was not yet established if the differences were caused by surface contamination or

inherent differences in the material structure. Auger analysis was performed on used samples of aluminum and gold. The results showed the presence of hydrocarbon on the surface with a thickness less than 2 nm; this might be the source of the variations.

Most of the yield data were fit well by power-law expression. The most notable discrepancy was for aluminum foil--the primary yield values at 1.74 keV, 2.64 keV and 4.1-5.4 keV most certainly deviated from a power-law fit. Measurements were repeated using different samples to ensure this was not an experimental error. Interestingly enough, calculations by Strickland do show good agreement with these results.

At x-ray energies below the Al K edge, the yields from aluminum foil and anodized aluminum were the same. This indicates that the thickness of the natural oxide layer is comparable to the electron ranges. On the other hand, the yields from silicon and glass differ significantly at low energies. This corresponds to a relatively thin oxide layer on the silicon.

Next, jump ratios $J(Y_p)$ across the absorption edges in the 1 to 6 keV range were derived from the measured primary yields. The yield values were extrapolated to the dominant absorption edges using the power-law fits. Absorption cross sections for compounds were calculated from weighted averages of the elements. The results are given in Table 1. These yield jump ratios are compared with the jump ratios $J(\mu)$ from published photoelectric absorption cross sections.

Table 1. Jump ratios of primary yields, $J(Y_p)$, and photoelectric cross sections, $J(\mu)$, across given edge energies

Photoemitter	Edge Energy	$J(Y_p)$	$J(\mu)$	$J(Y_p/J(\mu)$
Al_2O_3	1.56	2.8	3.46	0.81
Si	1.84	7.4	10.4	0.71
$C_2H_2Cl_2$	2.82	5.5	7.8	0.71
Ag	3.35	4.0	5.27	0.76
Ti	4.96	5.85	7.9	0.74

The ratios of the yield jumps to the absorption jumps, $J(Y_p)/J(\mu)$, were found to be nearly the same for all these materials. There are good reasons why the ratio of ratios are slightly lower for silicon and Saran. Undoubtedly, the experimental value of $J(Y_p)$ for Si was reduced by the thin oxide layer on the surface. Similarly, the calculated value of $J(\mu)$ for Saran did not take into account the lower percentage of chlorine owing to a greater carbon percentage from the plasticizer.

Now we turn our attention to secondary electrons. The measured values of the secondary-electron coefficient, $(Y_T-Y_p)/Y_p$, are given in Figure 9. Of the materials studied, the oxides of aluminum and silicon (glass) had the largest coefficients. The lowest coefficients were Mylar and silicon. This especially low secondary yield of Mylar is surprising since the yield from the other polymer tested, Saranwrap, was much higher. We do not have enough data yet to correlate secondary yields with the chemical composition. From some published work on secondary yields induced by electrons, there is an indication that the secondary yield decreases when the molecular structure is more complex. Research was begun to identify those polymers suitable for future studies.

As already stated, the magnetic spectrometer shown in Figures 4 and 5 was used to obtain preliminary primary-electron energy spectra. All features in the spectra are being correlated with the generation energies of photoelectrons and Auger electrons as part of the calibration studies. Studies were initiated to analyze the influence of surface contamination on these energy spectra. Empirical-analytic expressions are being developed to determine the energy-dependent electron ranges from the measured electron-energy spectra and from the energy-dependent yields.

Although steady-state measurements constitute most of the experimental work, some photoemission measurements were conducted using a pulsed x-ray source. These were done as an adjunct to diagnostic support for DNA-sponsored SGEMP programs. A set of seven x-ray diodes had photocathodes of different materials to determine the total photoemission yields. The most interesting finding of these limited studies was the apparently large difference in the secondary-electron coefficients of Kapton and Mylar. The total emission from Kapton was about twice that of Mylar even though they both have about the same average atomic weight and both polymers have chains of complex molecules.

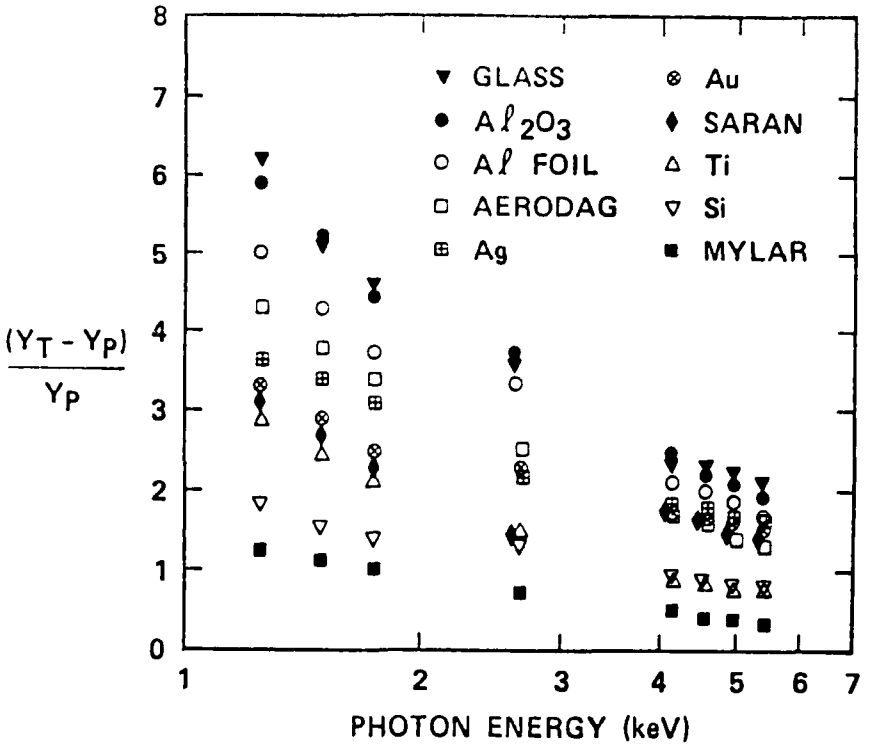

Figure 9. Secondary-electron coefficient: $Y_S/Y_P=(Y_T-Y_P)/Y_P$

PUBLICATIONS

1. M. J. Bernstein and J. A. Smith, "Primary and Secondary Photoelectron Yields Induced by Soft X Rays," accepted for publication in IEEE Trans. Nucl. Sci.

2. M. J. Bernstein and J. A. Smith, "X-Ray Response of a Channeltron Detector," manuscript in preparation for J. Appl. Phys. or Rev. of Sci. Instrum.

PRESENTATIONS AND INTERACTIONS

A talk entitled, "Primary and Secondary Photoelectron Yields Induced by Soft X Rays," was presented at the IEEE Conference on Nuclear and Space Radiation Effects in Santa Cruz, California, July 17-20, 1979.

Yield information learned from these studies was transmitted and discussed by mail and telephone with those doing related plasma-diagnostic-instrumentation calibrations including: J. Degnan (AFWL), R. Day (LASL), J. Gaines (LLL).